

# Numerical method for dc Josephson current between $d$ -wave superconductors

Yasuhiro Asano\*

Department of Applied Physics, Hokkaido University, Sapporo 060-8628, Japan

(Received 29 September 2000; published 17 January 2001)

We develop a numerical method to calculate the dc Josephson current between the  $d_{x^2-y^2}$ -wave superconductors. The Josephson junctions are described by the Bogoliubov–de Gennes equation on the two-dimensional tight-binding lattice. The Josephson current is expressed by the Matsubara Green function which is computed by the recursive Green-function method. We find in  $d$ -wave-superconductor/dirty-normal-metal/ $d$ -wave-superconductor junctions that the ensemble average of the Josephson current disappears for all temperature regimes when the angle between the crystal axis and the normal of the junction interface is  $\pi/4$ .

DOI: 10.1103/PhysRevB.63.052512

PACS number(s): 74.80.Fp, 74.25.Fy, 74.50.+r

In recent years, the Josephson effect between the anisotropic superconductors has attracted much attention because the high- $T_c$  superconductors might have  $d_{x^2-y^2}$ -wave pairing symmetry.<sup>1,2</sup> In anisotropic superconductors, the sign of the pair potentials depends on the direction of a quasiparticle's motion, which leads to the zero-energy states (ZES's) (Ref. 3) at the normal-metal/superconductor (NS) interface. The ZES's are detected in conductance spectra of  $N/I/d$ -wave superconductor junctions,<sup>4</sup> where  $I$  denotes the insulators. So far the dc Josephson effect has been discussed in  $dId$  junctions.<sup>5–9</sup> The critical Josephson current shows anomalous dependence on the temperature because of the ZES's. It is also shown that the roughness at the interface between the insulator and the superconductor suppresses the anomalous behavior.<sup>5,9</sup> The Josephson current also flows in systems such as  $dcd$  (Ref. 10) and  $dNd$  (Refs. 8, 11, and 12) junctions, where  $c$  is the constriction. The mesoscopic fluctuations of the critical current is one of the interesting topics when the normal metals is in the diffusive transport regime.<sup>13</sup>

In this paper, we present a numerical method to calculate the Josephson current between the two  $d$ -wave superconductors. The Josephson junction is described by the Bogoliubov–de Gennes equation<sup>14</sup> on the two-dimensional tight-binding model.<sup>15,16</sup> The Josephson current is represented by the Matsubara Green function<sup>17</sup> which is numerically calculated by using the recursive Green-function method.<sup>18</sup> The advantage of the method is wide applicability to various systems such as, the clean (ballistic) junctions, the dirty (diffusive) junctions, and the junctions in the localization regime.

Let us consider the  $dNd$  junction on the two-dimensional tight-binding model as shown in Fig. 1(a), where the length of the normal segment is  $La_0$  and the width of the junction is  $Wa_0$ , where  $a_0$  is the lattice constant. The pair potential in the momentum space is schematically depicted in the lower figures. In the  $d_{x^2-y^2}$ -wave superconductor, the  $a$  axis points the direction in which the amplitude of the pair potential takes its maximum. The orientation angle between the  $x$  direction and the  $a$  axis is  $\alpha_L$  and the phase of the pair potential is  $\phi_L$  in the superconductor on the left-hand side. On the right-hand side, they are  $\alpha_R$  and  $\phi_R$ , respectively. The Hamiltonian of the system reads

$$\begin{aligned}
 H = & -t \sum_{j=-\infty}^{\infty} \sum_{m=1}^W \sum_{\sigma} [c_{j+1,m,\sigma}^{\dagger} c_{j,m,\sigma} + \text{H.c.}] \\
 & -t \sum_{j=-\infty}^{\infty} \sum_{m=1}^W \sum_{\sigma} [c_{j,m+1,\sigma}^{\dagger} c_{j,m,\sigma} + \text{H.c.}] \\
 & + \sum_{j=-\infty}^{\infty} \sum_{m=1}^W \sum_{\sigma} (\epsilon_{j,m} + 4t - \mu) c_{j,m,\sigma}^{\dagger} c_{j,m,\sigma} \\
 & - \sum_{j',m'} \sum_{j,m} [\bar{\Delta}^*(j',m';j,m) c_{j',m',\uparrow} c_{j,m,\downarrow} + \text{H.c.}],
 \end{aligned} \tag{1}$$

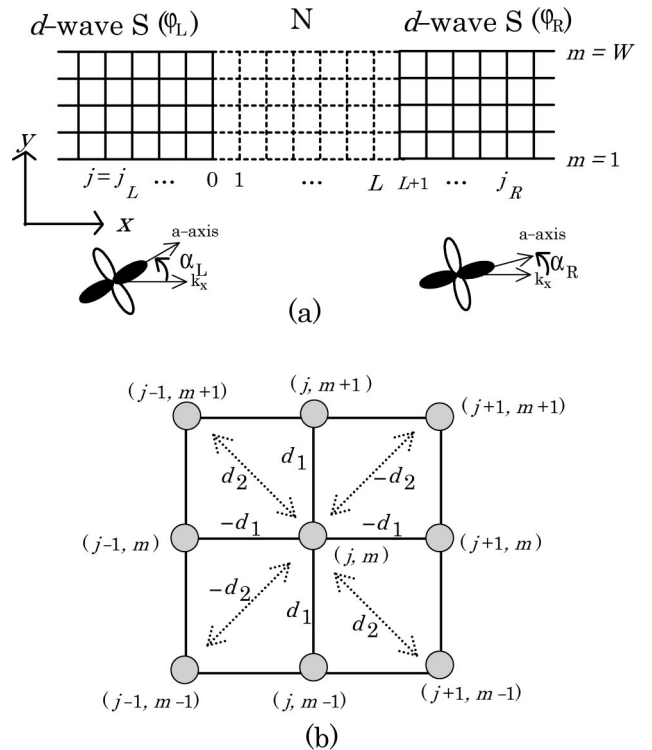


FIG. 1. The  $dNd$  junction is illustrated in (a). The orientation angle in the left (right) superconductor is  $\alpha_L$  ( $\alpha_R$ ). In (b), the pair potential in Eq. (6) is depicted on the tight-binding lattice.

where  $(j, m)$  is the lattice index,  $c_{j,m,\sigma}^\dagger$  ( $c_{j,m,\sigma}$ ) is the creation (annihilation) operator of an electron at  $(j, m)$  with spin  $\sigma$  ( $=\uparrow$  or  $\downarrow$ ),  $t$  is the nearest-neighbor hopping integral, and  $\mu$  is the Fermi energy, respectively. Throughout this paper, we take units of  $\hbar = k_B = 1$ , where  $k_B$  is the Boltzmann constant. In the  $y$  direction, the periodic boundary condition is applied. We assume that the on-site potential  $\epsilon_{j,m}$  is zero far from the interface in the two superconductors (i.e.,  $\epsilon_{j,m} = 0$  for  $j < j_L \leq 0$  and  $L+1 \leq j_R < j$ ). In the  $d$ -wave superconductor the pair potential  $\bar{\Delta}(\mathbf{R}, \mathbf{r} - \mathbf{r}')$  has the site-off-diagonal elements, where  $\mathbf{r} = (j, m)$ ,  $\mathbf{r}' = (j', m')$ ,  $\mathbf{R} = (\mathbf{r} + \mathbf{r}')/2$ , respectively. In what follows, we assume the uniform amplitude of the pair potential in the superconductors and neglect the dependence of  $\bar{\Delta}$  on  $\mathbf{R}$ . The pair potential is given in the Fourier representation

$$\bar{\Delta}(\mathbf{r} - \mathbf{r}', \alpha, \phi) = \frac{1}{(2\pi)^2} \int d\mathbf{k} \bar{\Delta}(\mathbf{k}, \alpha, \phi) e^{i\mathbf{k}(\mathbf{r} - \mathbf{r}')}. \quad (2)$$

In the case of the  $d_{x^2-y^2}$  symmetry, the Fourier component of the pair potential for  $\alpha = 0$  and  $\alpha = \pi/4$  can be described by

$$\bar{\Delta}(\mathbf{k}, 0, \phi) = 2\Delta e^{i\phi} (\cos k_y a_0 - \cos k_x a_0), \quad (3)$$

$$\bar{\Delta}(\mathbf{k}, \pi/4, \phi) = 2\Delta e^{i\phi} \sin k_x a_0 \sin k_y a_0, \quad (4)$$

where  $\Delta$  and  $\phi$  ( $=\phi_L$  or  $\phi_R$ ) are the amplitude and the phase of the pair potential, respectively. When  $-\pi/4 \leq \alpha \leq \pi/4$ , we describe the pair potential by the linear combination of Eqs. (3) and (4),

$$\bar{\Delta}(\mathbf{k}, \alpha, \phi) = \cos 2\alpha \bar{\Delta}(\mathbf{k}, 0, \phi) + \sin 2\alpha \bar{\Delta}(\mathbf{k}, \pi/4, \phi). \quad (5)$$

By substituting Eq. (5) into Eq. (2), the pair potential in real space results in

$$\begin{aligned} \bar{\Delta}(\mathbf{r} - \mathbf{r}', \phi, \alpha) = & -d_1 \delta_{|j'-j|,1} \delta_{m',m} + d_1 \delta_{j',j} \delta_{|m'-m|,1} \\ & - d_2 (\delta_{j',j+1} \delta_{m',m+1} + \delta_{j',j-1} \delta_{m',m-1}) \\ & + d_2 (\delta_{j',j+1} \delta_{m',m-1} + \delta_{j',j-1} \delta_{m',m+1}), \end{aligned} \quad (6)$$

$$d_1(\phi, \alpha) = \Delta e^{i\phi} \cos 2\alpha, \quad (7)$$

$$d_2(\phi, \alpha) = (\Delta/2) e^{i\phi} \sin 2\alpha. \quad (8)$$

The pair potential is schematically illustrated in Fig. 1(b). The Hamiltonian in Eq. (1) is diagonalized by the Bogoliubov transformation

$$\begin{bmatrix} c_{j,m,\uparrow} \\ c_{j,m,\downarrow}^\dagger \end{bmatrix} = \sum_{\nu} \begin{bmatrix} u_{\nu}(j,m) & -v_{\nu}^*(j,m) \\ v_{\nu}(j,m) & u_{\nu}^*(j,m) \end{bmatrix} \begin{bmatrix} \tilde{\gamma}_{\nu,\uparrow} \\ \tilde{\gamma}_{\nu,\downarrow}^\dagger \end{bmatrix}, \quad (9)$$

where  $\tilde{\gamma}_{\nu,\sigma}^\dagger$  ( $\tilde{\gamma}_{\nu,\sigma}$ ) is creation (annihilation) operator of a Bogoliubov quasiparticle. We omit the spin index of the wave function ( $u_{\nu}, v_{\nu}$ ) since we do not consider the spin-dependent potential in this study. The wave function satisfies the Bogoliubov–de Gennes equation in a matrix form

$$\check{T}_{j+1}^- \Psi_{\nu}(j+1) + \check{T}_j^+ \Psi_{\nu}(j-1) + \check{H}_j^0 \Psi_{\nu}(j) = E_{\nu} \Psi_{\nu}(j), \quad (10)$$

with

$$\check{T}_j^{\pm} = \begin{pmatrix} -t\hat{1} & \hat{\Delta}_2^{\pm}(j) \\ \hat{\Delta}_2^{\pm*}(j) & t\hat{1} \end{pmatrix}, \quad (11)$$

$$\check{H}_j^0 = \begin{pmatrix} \hat{h}_0(j) & \hat{\Delta}_1(j) \\ \hat{\Delta}_1^*(j) & -\hat{h}_0^*(j) \end{pmatrix}, \quad (12)$$

$$\begin{aligned} \hat{h}_0(j)|_{m,m'} = & \{\epsilon_{j,m} + 4t - \mu\} \delta_{m,m'} - t(\delta_{m,m'+1} + \delta_{m,m'-1}) \\ & - t(\delta_{m,1} \delta_{m',W} + \delta_{m,W} \delta_{m',1}), \end{aligned} \quad (13)$$

$$\begin{aligned} \hat{\Delta}_1(j)|_{m,m'} = & \bar{d}_1(j) (\delta_{m,m'+1} + \delta_{m,m'-1} + \delta_{m,1} \delta_{m',W} \\ & + \delta_{m,W} \delta_{m',1}), \end{aligned} \quad (14)$$

$$\begin{aligned} \hat{\Delta}_2^{\pm}(j)|_{m,m'} = & -d_1(j) \delta_{m,m'} \mp d_2(j) (\delta_{m,m'-1} + \delta_{m,1} \delta_{m',W}) \\ & \pm d_2(j) (\delta_{m,m'+1} + \delta_{m,W} \delta_{m',1}), \end{aligned} \quad (15)$$

$$\bar{d}_1(j) = \begin{cases} d_1(\phi_L, \alpha_L): & j \leq 0 \\ 0: & 1 \leq j \leq L \\ d_1(\phi_R, \alpha_R): & L+1 \leq j, \end{cases} \quad (16)$$

$$d_{1,2}(j) = \begin{cases} d_{1,2}(\phi_L, \alpha_L): & j \leq 0 \\ 0: & 1 \leq j \leq L+1 \\ d_{1,2}(\phi_R, \alpha_R): & L+2 \leq j. \end{cases} \quad (17)$$

Here  $E_{\nu}$  is the eigenvalue measured from the chemical potential of the junction. The wave function  $\Psi_{\nu}(j)$  is the vector with  $2W$  components and  $m$ th ( $m+W$ th) component is  $u_{\nu}(j, m)$  [ $v_{\nu}(j, m)$ ]. The  $W \times W$  ( $2W \times 2W$ ) matrices are indicated by  $\hat{\Delta}$  ( $\check{\Delta}$ ) and the unit matrix is denoted by  $\hat{1}$ . The Matsubara Green function is defined by

$$\check{G}_{\omega_n}(j, j') = \sum_{\nu} \frac{\Psi_{\nu}(j) \Psi_{\nu}^{\dagger}(j')}{i\omega_n - E_{\nu}}, \quad (18)$$

where  $\omega_n = (2n+1)\pi T$  and  $T$  are the Matsubara frequency and the temperature, respectively.

The Josephson current in the normal region ( $1 \leq j \leq L$ ) is derived from the current conservation law

$$\frac{\partial}{\partial \bar{t}} e \sum_{m,\sigma} \langle c_{j,m,\sigma}^{\dagger}(\bar{t}) c_{j,m,\sigma}(\bar{t}) \rangle + J(j) - J(j-1) = 0, \quad (19)$$

$$J(j) = -ieT \sum_{\omega_n} t \text{Tr}[\check{G}_{\omega_n}(j+1, j) - \check{G}_{\omega_n}(j, j+1)], \quad (20)$$

where  $\bar{t}$  and  $\langle \dots \rangle$  denote the time and the thermal average, respectively. In the dc Josephson effect, we note that  $J(j)$  is independent of  $j$  because the first term in Eq. (19) becomes

zero. When we calculate the current in the superconductors, the source term proportional to the order parameter must be added in Eq. (20).<sup>17</sup>

In order to calculate the Green function in Eq. (20), we apply the recursive Green-function method.<sup>18</sup> First we calculate the two initial Green functions  $\check{G}_{j_L}^{\mathcal{L}}$  and  $\check{G}_{j_R+1}^{\mathcal{R}}$  for fixed Matsubara frequency. Here  $\check{G}_{j_0}^{\mathcal{L}(\mathcal{R})} \equiv \check{G}_{\omega_n}^{\mathcal{L}(\mathcal{R})}(j_0, j_0)$  is the Green function of a system in which all lattice sites  $j \geq j_0 + 1$  ( $j \leq j_0 - 1$ ) are deleted. Next we calculate  $\check{G}_{j_N-1}^{\mathcal{L}}$  and  $\check{G}_{j_N+1}^{\mathcal{R}}$  for  $1 < j_N < L$  by obeying the recursive formula

$$\check{G}_j^{\mathcal{L}} = [i\omega_n \check{I} - \check{H}_j^0 - \check{T}_j^+ \check{G}_{j-1}^{\mathcal{L}} \check{T}_j^-]^{-1}, \quad (21)$$

$$\check{G}_j^{\mathcal{R}} = [i\omega_n \check{I} - \check{H}_j^0 - \check{T}_{j+1}^- \check{G}_{j+1}^{\mathcal{R}} \check{T}_{j+1}^+]^{-1}, \quad (22)$$

starting from  $j = j_L$  in Eq. (21) and  $j = j_R$  in Eq. (22), respectively. The Green function  $\check{G}_{\omega_n}^{\mathcal{L}(\mathcal{R})}(j_N, j_N)$  is computed by using the formula

$$\check{G}_{\omega_n}^{\mathcal{L}(\mathcal{R})}(j, j) = [i\omega_n \check{I} - \check{H}_j^0 - \check{T}_{j+1}^- \check{G}_{j+1}^{\mathcal{R}(\mathcal{L})} \check{T}_{j+1}^+ - \check{T}_j^+ \check{G}_{j-1}^{\mathcal{L}(\mathcal{R})} \check{T}_j^-]^{-1}, \quad (23)$$

for  $j = j_N$ . Then we obtain the off-diagonal Green functions in Eq. (20) by the relations

$$\check{G}_{\omega_n}^{\mathcal{L}}(j+1, j) = \check{G}_{j+1}^{\mathcal{R}} \check{T}_{j+1}^+ \check{G}_{\omega_n}^{\mathcal{L}}(j, j), \quad (24)$$

$$\check{G}_{\omega_n}^{\mathcal{R}}(j, j+1) = \check{G}_{\omega_n}^{\mathcal{L}}(j, j) \check{T}_{j+1}^- \check{G}_{j+1}^{\mathcal{R}}, \quad (25)$$

for  $j = j_N$ . Finally the Josephson current is calculated by carrying out the summation with respect to the Matsubara frequency. Here we briefly mention the method to calculate initial Green functions (i.e.,  $\check{G}_{j_L}^{\mathcal{L}}$  and  $\check{G}_{j_R+1}^{\mathcal{R}}$ ). The initial Green functions can be obtained analytically for the *s*-wave superconductor.<sup>17</sup> In the case of *d*-wave superconductor for  $\alpha \neq 0$ , however, it seems to be difficult to derive an analytic expression. In this paper, we apply a numerical method which was used to obtain the initial Green function in the uniform magnetic field.<sup>19</sup> In this method, it is possible to calculate numerically the initial Green function when the system under consideration has the translational symmetry in the *x* direction. In the original paper,<sup>19</sup> the retarded Green function is computed. It is possible to apply the method to the Matsubara Green function without any difficulty.

At first we apply the present method to *dId* junctions in order to check the validity of the method. In Fig. 2(a), we show the calculated results of the Josephson critical current as a function of the temperature for several choices of  $(\alpha_L, \alpha_R)$ , where  $L = 5$ ,  $W = 20$ ,  $\mu = 1.0t$ , and  $R_j$  is the resistance of the junction, respectively. We assume that the dependence of  $\Delta$  on the temperature is described by the BCS theory and the critical temperature is  $T_c \sim 0.57\Delta_0$ , where  $\Delta_0$  is the amplitude of the pair potential at  $T = 0$  and is  $0.1t$  in Fig. 2. In the normal segment, the barrier potential is chosen to be  $\epsilon_{j,m} = 4.0t$  for  $1 \leq j \leq L$ . In these parameters, the Josephson current is proportional to  $\sin(\phi_R - \phi_L)$ . The results for  $(\alpha_L, \alpha_R) = (0, 0)$  show the saturation in the limit of  $T$

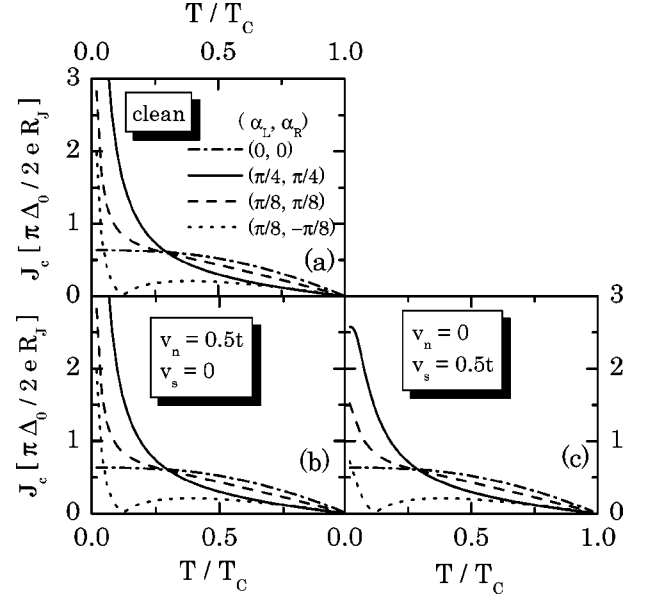


FIG. 2. The critical Josephson current in *dId* junctions is plotted as a function of the temperature for several choices of  $(\alpha_L, \alpha_R)$ . In (a), the calculated results for clean *dId* junctions are shown. In (b) and (c), we consider the roughness at the interface between the *d*-wave superconductor and the insulator. The random potential is introduced on the insulator side in (b). On the other hand, in (c), the random potential is introduced on the superconductor side.

$\rightarrow 0$ . The results for  $(\alpha_L, \alpha_R) = (\pi/8, \pi/8)$  and  $(\pi/4, \pi/4)$  increase sharply with decreasing the temperature because of the ZES at the interface. In the case of  $(\alpha_L, \alpha_R) = (\pi/8, -\pi/8)$ , the Josephson current changes its sign around  $T/T_c \sim 0.12$ . The ZES is a source of the sign change in the Josephson current. The present numerical method reproduces the characteristic behavior of the Josephson current in the previous works.<sup>5-9</sup> We consider the roughness at the interface between the insulator and the superconductor in Figs. 2(b) and (c). The potentials at  $j = 1$  and  $L$  are described by  $\epsilon_{j,m} = 4.0t + \tilde{v}_{j,m}$ , where  $\tilde{v}_{j,m}$  are given randomly in the range of  $-v_n/2 \leq \tilde{v}_{j,m} \leq v_n/2$ . In the same way, the potential at  $j = -1$  and  $L+1$  are given randomly in the range of  $-v_s/2 \leq \epsilon_{j,m} \leq v_s/2$ . In Fig. 2(b), we introduce the interfacial roughness on the insulator side, (i.e.,  $v_n = 0.5t, v_s = 0$ ). The characteristic behavior of the Josephson current is almost the same with that in the clean *dId* junction in Fig. 2(a). On the other hand in Fig. 2(c), the roughness is introduced on the superconductor side, (i.e.,  $v_n = 0, v_s = 0.5t$ ). In the limit of  $T \rightarrow 0$ , the singular behavior in  $J_c$  is suppressed because the ZES is broadened due to the roughness at the interface.<sup>5</sup> Since the ZES is localized at the interface on the superconductor side, the random potential in the superconductor suppresses the low-temperature anomaly.

Next we apply the method to dirty *dNd* junctions. In Fig. 3, we show the Josephson current at  $\phi_R - \phi_L = \pi/2$  as a function of the temperature, where  $L = 70$ ,  $W = 20$ , and  $\Delta_0 = 0.01t$ , respectively. The results for  $(\alpha_L, \alpha_R) = (0, 0)$  and  $(\pi/4, \pi/4)$  are shown in (a) and (b), respectively. We introduce the barrier potential at the interface,  $\epsilon_{j,m} = 4t$  for  $j = 1$  and  $L$ , and the random potential in the normal segment,

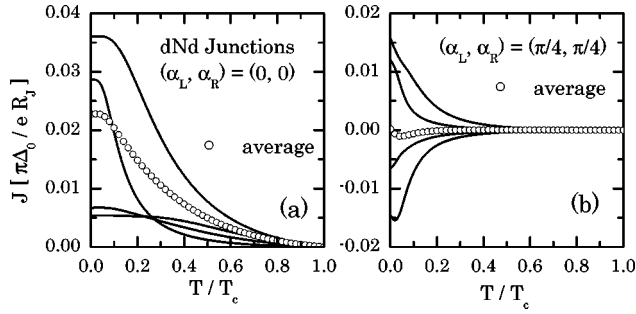


FIG. 3. The Josephson current in dirty- $dNd$  junction is plotted as a function of the temperature for  $(\alpha_L, \alpha_R) = (0, 0)$  in (a) and  $(\pi/4, \pi/4)$  in (b), respectively. The lines are the results of several samples with different random configurations and the open circles are the ensemble average over ten samples.

$-v_n/2 \leq \epsilon_{j,m} \leq v_n/2$  for  $2 < j < L-1$ . The mean free path and the localization length in the normal conductor are about  $6.8a_0$  and  $59a_0$ , respectively. In the present method, it is possible to calculate the Josephson current of a single sample with specific random configuration. This is one of the advantages of the present method because the Josephson current of a specific sample in the simulation corresponds to that of a specific sample in experiments. The ensemble average of the Josephson current is obtained from the results in a number of samples with different random configuration. In Fig. 3, the lines represent the calculated results of several different samples and the open circles denote the ensemble average over ten samples. The ensemble average of  $J$  for  $(\alpha_L, \alpha_R) = (0, 0)$  remains finite value as shown in Fig. 3(a). The sample-to-sample fluctuations exist in the Josephson current<sup>13</sup> as shown with the lines. On the other hand for

$(\pi/4, \pi/4)$ , the ensemble average of  $J$  almost vanishes for all temperature regime as shown in Fig. 3(b). The amplitudes of the sample-specific Josephson current, however, remain finite values for  $T/T_c < 0.5$  and show the rapid increase with decreasing the temperature as well as those in the  $dId$  junctions. The sign of the Josephson current can be either positive or negative depending on the random configurations. The results indicate an importance of the mesoscopic fluctuations in the Josephson current. The fluctuations in  $d$ -wave junctions increase with decreasing  $T$  because of the ZES at the  $NS$  interface in contrast to those in the  $s$ -wave junctions, where the fluctuations saturate in the limit of  $T \rightarrow 0$ . The  $d$ -wave pairing symmetry of the superconductor is responsible for the disappearance of the averaged Josephson current for  $(\pi/4, \pi/4)$ . It is possible to show that the ZES's do not contribute to the ensemble average of the Josephson current in an analytic calculation. The details will be given elsewhere.

In summary, we presented a numerical method for the Josephson current between two  $d$ -wave superconductors. The Josephson current is calculated from the Matsubara Green function of the Bogoliubov-de Gennes equation. The Green function is computed by using the recursive Green-function method. The low-temperature anomaly of the Josephson current in  $dId$  junctions is reproduced in the present method. In dirty- $dNd$  junctions, the ensemble average of the Josephson current vanishes when the orientation angle is  $(\alpha_L, \alpha_R) = (\pi/4, \pi/4)$ . This fact, however, does not mean the disappearance of the critical current in experiments because the sample-specific critical current remains finite value.

The author is indebted to N. Tokuda, H. Akera, and Y. Tanaka for useful discussion.

\*Email address: asano@eng.hokudai.ac.jp

<sup>1</sup>M. Sigrist and T.M. Rice, J. Phys. Soc. Jpn. **61**, 4283 (1992); Rev. Mod. Phys. **67**, 503 (1995).

<sup>2</sup>D.A. Wollman, D.J. van Harlingen, W.C. Lee, D.M. Ginsberg, and A.J. Leggett, Phys. Rev. Lett. **71**, 2134 (1993).

<sup>3</sup>C.R. Hu, Phys. Rev. Lett. **72**, 1526 (1994).

<sup>4</sup>I. Iguchi, W. Wang, M. Yamazaki, Y. Tanaka, and S. Kashiwaya, Phys. Rev. B **62**, R6131 (2000); Y. Tanaka and S. Kashiwaya, Phys. Rev. Lett. **74**, 3451 (1995).

<sup>5</sup>Y.S. Barash, H. Burkhardt, and D. Rainer, Phys. Rev. Lett. **77**, 4070 (1996).

<sup>6</sup>Y. Tanaka and S. Kashiwaya, Phys. Rev. B **56**, 892 (1997).

<sup>7</sup>M.P. Samanta and S. Datta, Phys. Rev. B **55**, R8689 (1997).

<sup>8</sup>R.A. Riedel and P.F. Bagwell, Phys. Rev. B **57**, 6084 (1998).

<sup>9</sup>A.A. Golubov and M.Y. Kupriyanov, Pis'ma Zh. Éksp. Teor. Fiz. **69**, 242 (1999) [JETP Lett. **69**, 262 (1999)].

<sup>10</sup>M. Fogelstöm, S. Yip, and J. Kurkijärvi, Physica C **294**, 289 (1998).

<sup>11</sup>W. Zhang, Phys. Rev. B **52**, 3772 (1995).

<sup>12</sup>J.-X. Zhu, Z.D. Wang, and H.X. Tang, Phys. Rev. B **54**, 7354 (1996).

<sup>13</sup>B.L. Al'tshuler and B.Z. Spivak, Zh. Éksp. Teor. Fiz. **65**, 609 (1987) [Sov. Phys. JETP **65**, 343 (1987)].

<sup>14</sup>P.G. de Gennes, *Superconductivity of Metals and Alloys* (Benjamin, New York, 1966).

<sup>15</sup>Y. Tanuma, Y. Tanaka, M. Yamashiro, and S. Kashiwaya, Phys. Rev. B **57**, 7997 (1998).

<sup>16</sup>J.-X. Zhu and C.S. Ting, Phys. Rev. B **61**, 1456 (2000).

<sup>17</sup>A. Furusaki, Physica B **203**, 214 (1994).

<sup>18</sup>P.A. Lee and D.S. Fisher, Phys. Rev. Lett. **47**, 882 (1981).

<sup>19</sup>T. Ando, Phys. Rev. B **44**, 8017 (1991).